Master in Medical Imaging and Applications

Medical Image Segmentation and Applications (MISA): IBSR18 PROJECT

Authors:
Katherine Sheran
Umamaheswaran Raman Kumar

Professors:
Xavier Llado
Robert Marti

Lab instructor:
Jose Bernal

January 19, 2018

Contents

1 Introduction **3**

1.1 Context . . . 3

1.2 Problem definition . . . 3

1.3 Project goal . . . 4

1.4 Materials . . . 4

2 Methodology **5**

2.1 Atlas Based Approach . . . 5

2.1.1 Pre-processing . . . 6

2.1.2 Segmentation . . . 6

2.1.3 Post-processing . . . 7

2.2 SPM 12 . . . 7

2.3 Evaluation metrics . . . 8

2.3.1 Primary metrics . . . 8

2.3.2 Secondary metrics . . . 9

3 Design and Implementation **11**

3.1 Atlas Based Segmentation . . . 11

3.1.1 Implementation Steps . . . 11

3.1.2 Implementation Files . . . 12

3.2 SPM 12 . . . 13

3.2.1 Realign Function . . . 14

3.2.2 Segment Function . . . 15

4 Experiments **17**
4.1 Atlas based segmentation . . . 17
4.1.1 Test Runs . . . 17
4.2 SPM12 segmentation . . . 22
4.2.1 Test Runs . . . 22

5 Results **27**
5.1 Quantitative results . . . 27
5.1.1 Dice Coefficient . . . 27
5.1.2 Hausdorff Distance . . . 28
5.1.3 Average Distance . . . 28
5.1.4 Jaccard Coefficient . . . 28
5.1.5 False Positive Error . . . 29
5.1.6 False Negative Error . . . 29
5.1.7 Volume Similarity . . . 29
5.2 Qualitative results . . . 30
5.2.1 Segmentation Results - ITK Snap . . . 30
5.2.2 Segmentation Volume Overlay - Slicer 3D . . . 33
5.2.3 Squared difference image . . . 35
5.3 Discussions . . . 38

6 Project Management **39**

7 Conclusions **41**

1. Introduction

1.1 Context

Magnetic resonance imaging (MRI) of the brain is a non-invasive and painless imaging technology that produces three dimensional detailed anatomical images of the brain without the use of damaging radiation. It has become a standard tool in neurology for diagnosis, treatment monitoring and disease follow up.

Brain structure segmentation in MRI is of great interest in medical practice due to its various applications, including pre-operative evaluation, surgical planning, radiotherapy treatment planning, longitudinal monitoring for disease progression or remission [Phillips 2015]. Manual segmentation of brain MRI suffers from important shortcomings, as the segmentations are poorly reproducible, subject to inter- and intra-operator variability and most importantly, it has proven to be a highly time consuming task.

1.2 Problem definition

The development of robust automated methods for brain segmentation capable of segmenting large amounts of data in a short time and that is highly reproducible is an active research field in medical imaging. However due to noise, difference in tissue intensities, partial volume effects [Akselrod-Ballin 2007], or the absence of anatomic models that fully capture the possible deformations in each structure [Kapur 1996], automatic brain segmentation still remains a challenging problem in medical imaging.

1.3 Project goal

The goal of this project is to develop an automatic tissue segmentation method for segmenting MRI brain images into three classes: White Matter (WM), Gray Matter (GM) and cerebrospinal fluid (CSF).

The proposed algorithm will be evaluated based on Dice Similarity Coefficient (DSC), Hausdorff distance (HD) and average volumetric difference (AVD).

1.4 Materials

The proposed solution will be evaluated on the IBSR18 data set. This is one of the standard data sets for tissue quantification and segmentation evaluation. As its name indicates, the data set consists of 18 MRI volumes, skull-stripped, T1-w images and contains cases with different spatial resolutions. Moreover, there is also a heterogeneity in image intensities which hinders segmentation. The original set has been divided into:

- Training: 10 images + ground truth
- Validation: 5 images + ground truth
- Testing: 3 images (no ground truth)

2. Methodology

In this section we propose two different methods for performing the automatic brain segmentation task. The first method, Atlas based segmentation, was seen during the course and implemented on a previous lab. This previous implementation was used as a starting point and further improved in order to provide better segmentation results. The second method, consisted on using SPM. SPM stands for Statistical Parametric Mapping and consists on a software package that has been specially designed for the analysis of brain imaging data sequences. The software provides several tools, for registration, smoothing, bias field correction and segmentation of brain images.

2.1 Atlas Based Approach

In the context of image segmentation, an atlas is defined as the combination of two image volumes: one intensity image (or template) and one segmented image (or labeled image). Probabilistic or statistical atlases are constructed on the basis of populations, co-registering all the segmented cases to a standard space and computing the frequency of each voxel to belong to a specific structure [Cabezas 2011]. For this project we have chosen to implement a probabilistic atlas for performing the brain tissue segmentation. Figure 2.1 displays the main steps of the proposed atlas based segmentation approach.

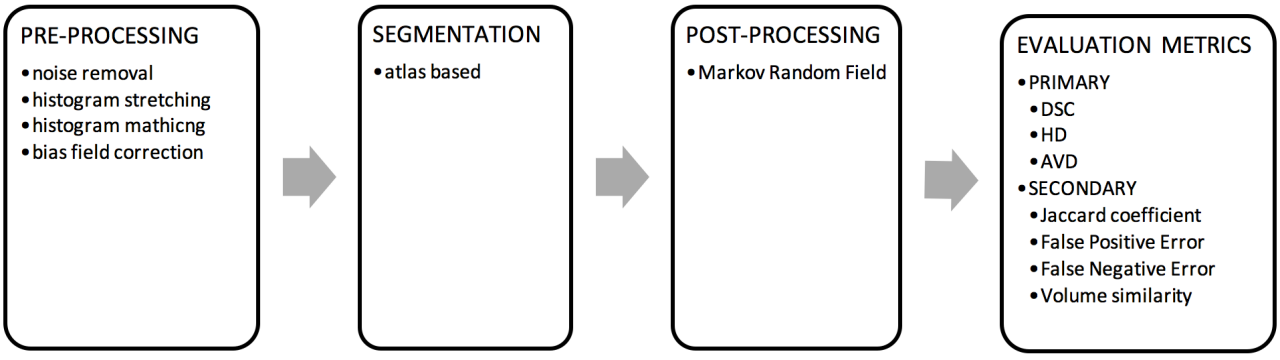

Figure 2.1: Block diagram of the atlas based segmentation approach

2.1.1 Pre-processing

During MR image acquisition, different scanners or parameters would be used for scanning different subjects or the same subject at a different time, which may result in large intensity variations. This intensity variation will greatly undermine the performance of subsequent MRI processing and population analysis, such as image registration, segmentation, and tissue volume measurement [Sun 2015].

Noise Removal

Anisotropic diffusion, is a technique aiming at reducing image noise without removing significant parts of the image content, typically edges, lines or other details that are important for the interpretation of the image [Perona 1990].

Histogram Stretching

Contrast stretching (often called normalization) is a simple image enhancement technique that attempts to improve the contrast in an image by stretching the range of intensity values it contains to span a desired range of values, e.g. the the full range of pixel values that the image type concerned allows [Jain 1989].

Histogram Matching

Histogram matching or histogram specification is the transformation of an image so that its histogram matches a specified histogram [Gonzalez 2002]. This technique helps reduce the intensity variation between MRIs obtained from different acquisitions.

Bias Field correction

Bias field signal is a low-frequency and very smooth signal that corrupts MRI images. It affects the intensities of the homogeneous tissue regions (GM, WM and CSF). Therefore, the bias field signal needs to be corrected before submitting the corrupted MRI images to a segmentation algorithm.

2.1.2 Segmentation

As mentioned before, segmentation can be a challenging task due to problems linked to low contrast images, fuzzy object contours, similar intensities with adjacent objects of interest, among others. Therefore, having a prior knowledge can be of great help for improving

the segmented results [Cuadra 2015]. One of the techniques that aids on extracting prior knowledge for performing a better segmentation is an atlas. A basic atlas is a combination of an intensity image (template) and its segmented image (labels). After registering the atlas template and the target image, the atlas labels are propagated to the target image, resulting in an atlas based segmentation. Atlases bring useful prior information to segmentation and registration tasks, so that variation within population can be described with fewer transformation parameters [Kalinić 2009].

2.1.3 Post-processing

Markov Random Field

A natural way of incorporating spatial correlations into a segmentation process is to use Markov random fields (MRF) as a priori models. The MRF is a stochastic process that specifies the local characteristics of an image and is combined with the given data to reconstruct the true image. The MRF of prior contextual information is a powerful method for modeling spatial continuity and other features, and even simple modeling of this type can provide useful information for the segmentation process [Held 1997].

2.2 SPM 12

Statistical Parametric Mapping refers to the construction and assessment of spatially extended statistical processes used to test hypotheses about functional imaging data. These ideas have been instantiated in a software that is called SPM. SPM is an open source software developed in MATLAB environment by the Wellcome Department of Imaging Neuroscience at University College in London. The SPM software package has been designed for the analysis of brain imaging data sequences. The sequences can be a series of images from different cohorts, or time-series from the same subject. The current version of the software is SPM12.

The algorithm present in SPM12 is basically a probabilistic brain segmentation framework based on GMM with prior atlas information. Brain tissue distributions are estimated by a Gaussian Mixture Model where prior tissue probabilities are obtained registering a probabilistic atlas into the input to obtain the initial tissue probabilities for each tissue. The method aggregates the combination of image registration, tissue classification and bias correction in the same time by a derivation of the log-likelihood function [Ashburner 2005].

The program permits several output configurations options for segmented tissue: White Matter (WM), Gray Matter (GM), cerebrospinal fluid (CSF), bone, soft tissue and air/background (BGND). It also allows the user to modify the intensity of the bias field correction (no regularisation, light, medium, heavy). By default segmented images are aligned with the input image, but it is also possible to align the output images with the prior atlas to produce normalized segmentation to be used in other processes.

.

2.3 Evaluation metrics

In this section we present the evaluation metrics that have been used to evaluate the performance of our proposed segmentation algorithm. They have been divided into primary and secondary metrics. Primary metrics (DSC, HD, AVD) are the ones required for the evaluation of this project. Whereas secondary metrics are additional metrics that we decided to include in order to better assess our performance.

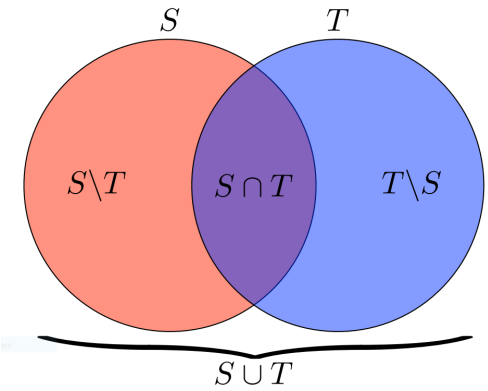

Figure 2.2: Venn diagram for understanding overlapping measures[Tustison 2009].

2.3.1 Primary metrics

Dice Coefficient

Dice Similarity Coefficient (DSC) measures the overlap of the segmentation with the ground-truth on a scale between 0 and 1. The former meaning 0 overlap and the latter meaning a 100% overlap with the ground-truth. Equation 2.1 shows how to compute the DSC.

$$DSC = 2\frac{\mid S_r \cap T_r \mid}{\mid S_r \mid + \mid T_r \mid} \tag{2.1}$$

Hausdorff Distance

Hausdorff Distance (HD) is the maximum distance from all the minimum distances between boundaries of segmentation and boundaries of the ground-truth. This spatial distance based metric is defined as a function of the Euclidean distances between the voxels of Sr and Tr as shown in 2.2

$$HD(Sr, Tr) = max(h(Sr, Tr), h(Tr, Sr)) \tag{2.2}$$

$$h(Sr, Tr) = max_{s \in Sr} min_{t \in Tr} ||s - t|| \tag{2.3}$$

Average Distance

The Average Distance (AVD) is defined as the average of minimum distances from points in the first set to the points in the second set and viceversa [Taha 2015]. It can be computed as shown in Equation 2.4:

$$AVD(Sr, Tr) = \frac{d(Sr, Tr) + d(Tr, Sr)}{2} \tag{2.4}$$

where $d(Sr, Tr)$ is the directed average Hausdorff distance that is given by:

$$d(Sr, Tr) = \frac{1}{N} \sum_{x \in Sr} min_{y \in Tr} ||x - y|| \tag{2.5}$$

2.3.2 Secondary metrics

Jaccard Coefficient

The Jaccard similarity index measures the overlap between the segmentation results and the ground truth [Jaccard 1912]. It is defined as the intersection between the two sets, divided by their union as shown in Equation 2.6:

$$JC = 2 \frac{\mid S_r \cap T_r \mid}{\mid S_r \cup T_r \mid} \tag{2.6}$$

False Positive Error

A false positive rate, also called Fallout, is a result that indicates that a given condition exists, when in reality it does not. In brain tissue segmentation this would mean affirming that pixel corresponds to a certain tissue type when in reality it is wrongly labeled. The false positive error can be compute with Equation 2.7:

$$FP = \frac{\mid S_r \setminus T_r \mid}{\mid S_r \mid} \tag{2.7}$$

False Negative Error

A false negative error is a result that indicates that a condition does not hold, while in fact it does. It is computed as shown in Equation 2.8:

$$FN = \frac{\mid T_r \setminus S_r \mid}{\mid T_r \mid} \tag{2.8}$$

Volume Similarity

As the name implies, volumetric similarity (VS) is a measure that considers the volumes of the segments to indicate similarity. Computing the volume similarity gives a result between -1 and 1. The former meaning that the result is underestimated and the latter, meaning that it is overestimated. Whereas a value of 0 indicates that both images have the same volume. This computation was done using Equation 2.9:

$$VS = 2\frac{\mid S_r \mid - \mid T_r \mid}{\mid S_r \mid + \mid T_r \mid} \tag{2.9}$$

3. Design and Implementation

3.1 Atlas Based Segmentation

3.1.1 Implementation Steps

This section provides the steps involved in the implementation of atlas based segmentation approach explained in the previous section:

- ***Step 1 (Matlab) :*** Normalize the intensity of training volume *IBSR_07* in the range of *0 - 200* as this volume will be used for the histogram matching step.
- ***Step 2 (ITK) :*** Apply anisotropic diffusion denoising to all the volumes in the dataset using the *itk::CurvatureAnisotropicDiffusionImageFilter* class from ITK with *TimeStep* 0.05, *NumberOfItertions* 2 and *ConductanceParameter* 3.0. For this step it is required that the input images are type casted to float using the *itk::CastImageFilter* class.
- ***Step 3 (ITK) :*** Apply histogram matching to all the volumes in the dataset using the *itk::HistogramMatchingImageFilter* class from ITK with the *ReferenceImage* as *IBSR_07*, *NumberOfHistogramLevels* 256, *NumberOfMatchingPoints* 7 and the *ThresholdAtMeanIntensity* flag *Set*.
- ***Step 4 (Matlab) :*** Register all the training volumes and its corresponding label volumes to one reference frame *IBSR_01*. First a rigid registration is applied followed by a non-rigid B-spline registration to obtain the final registered output volumes. The transformation obtained from the registration is applied to its corresponding label volumes to get the transformed label volumes. This process is done iteratively and all the registered training intensity volumes and label volumes are stored in a folder named *'registered'* inside the training volumes folder.
- ***Step 5 (Matlab) :*** Generate the probabilistic atlas volumes *P(X)* and intensity models *P(Y/X)* from the registered training volumes. The 4 atlas volumes corresponding to background, CSF(Cerebrospinal fluid), GM(Gray Matter) and WM(White

Matter), the intensity models *.mat* file and the template volume *IBSR_01* are stored in a folder named *'atlas'* inside the *'registered'* folder created in the previous step.

- ***Step 6 (Matlab) :*** Register the template volume to the test intensity volume to be segmented and transform all the atlas volumes to the test volume reference frame by using the transformation parameters obtained from registration.
- ***Step 7 (Matlab) :*** Find the post probability of each voxel of the test intensity volume using the transformed probabilistic atlas, $P(X)$ and the tissue model, $P(Y/X)$.
- ***Step 8 (Matlab) :*** After calculating the post probabilities for all the classes, the class with the maximum post probability at each voxel is assigned the class label in the final segmented volume.
- ***Step 9 (ITK) :*** Calculate the primary and secondary metrics to compare segmentation results incase of validation set. All the metrics are calculated using ITK class *itk::LabelOverlapMeasuresImageFilter* except for HD and AVD which are calculated using *itk::HausdorffDistanceImageFilter*.

3.1.2 Implementation Files

Most of the pre-processing and metrics calculation was implemented using ITK and the atlas method was implemented using Matlab. The files required for executing different steps are provided in the below mentioned folder structure:

- ***Step 1***
  - *1-Preprocessing -> Matlab -> F1_NormalizeVolume.m*
- ***Step 2 & 3***
  - *1-Preprocessing -> C++ -> MISAProject.pro*
  - *1-Preprocessing -> C++ -> main.cpp*
- ***Step 4***
  - *2-Segmentation -> Matlab -> F2_CreateRegisteredVolumes.m*
  - *2-Segmentation -> Matlab -> elastix -> elastixregister.bat*
  - *2-Segmentation -> Matlab -> elastix -> elastixtransform.bat*
  - *2-Segmentation -> Matlab -> elastix -> parameters_Rigid.txt*

  - *2-Segmentation -> Matlab -> elastix -> parameters_BSpline.txt*

- ***Step 5***
  - *2-Segmentation -> Matlab -> F3_BuildProbabilisticAtlas.m*

- ***Step 6, 7 & 8***
  - *2-Segmentation -> Matlab -> F4_ValidationResults.m*
  - *2-Segmentation -> Matlab -> F4_TestResults.m*
  - *2-Segmentation -> Matlab -> fn_atlas_segmentation.m*
  - *2-Segmentation -> Matlab -> fn_dice_similarity.m*
  - *2-Segmentation -> Matlab -> elastix -> elastixregister.bat*
  - *2-Segmentation -> Matlab -> elastix -> elastixtransform.bat*
  - *2-Segmentation -> Matlab -> elastix -> parameters_Rigid.txt*
  - *2-Segmentation -> Matlab -> elastix -> parameters_BSpline.txt*

- ***Step 9***
  - *3-Results -> C++ -> HausdorffDistance -> HausdorffDistance.pro*
  - *3-Results -> C++ -> HausdorffDistance -> main.cpp*
  - *3-Results -> C++ -> StapleGui folder*

- ***Post processing***
  - *4-Postprocessing -> MarkovRandomField-InProgress -> MISAMRF.pro*
  - *4-Postprocessing -> MarkovRandomField-InProgress -> main.cpp*

3.2 SPM 12

As previously explained, Statistical Parametric Mapping refers to the construction and assessment of spatially extended statistical processes used to test hypotheses about functional imaging data. These ideas have been instantiated in an open source software for Matlab that is called SPM which can be downloaded from: http://www.fil.ion.ucl.ac.uk/spm/

The SPM software package has been designed for the analysis of brain imaging data sequences. The current version of SPM is SPM12 which contains substantial theoretical, algorithmic, structural and interface enhancements over its previous versions. Moreover,

the current release has been designed for the analysis of fMRI, PET, SPECT, EEG and MEG.

In general terms the SPM12 software can be divided into three main sections: (1) spatial pre-processing functions, (2) statistical functions and (3) visualization functions. These sections can be clearly identified on Figure 3.1.

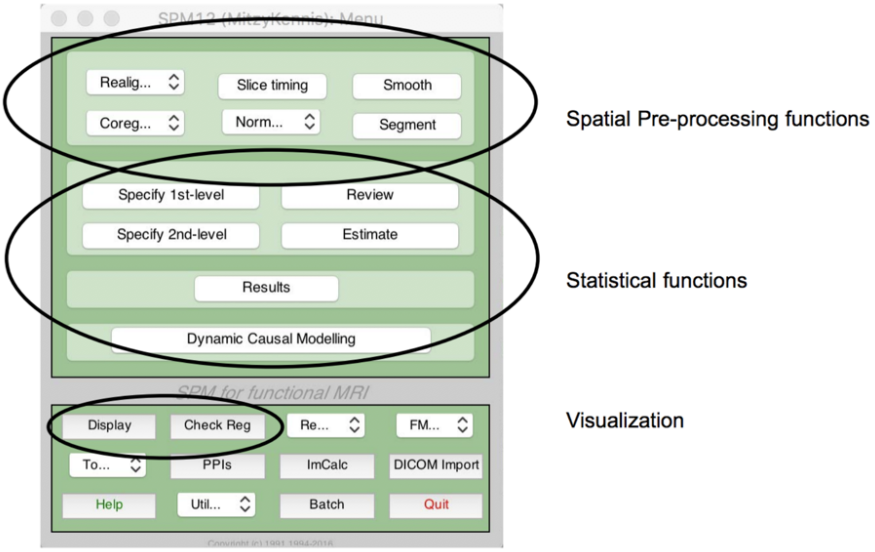

Figure 3.1: Main menu and sections of SPM12

For our segmentation problem we have mainly used two steps from the spatial pre-processing functions of SPM12: (1) Realign and (2) Segment. These steps are further explained on the section below.

3.2.1 Realign Function

Realign is the most basic function to match images. It uses a rigid body transformation to manipulate the MR scans. This means that it allows only translations and rotations (over the X, Y, and Z axis). By trial and error it tries to find the manipulation that minimizes the difference between two scans. The minimized cost function is the sum of squared differences between the two scans. As a consequence, it can only be used within scans that have been acquired with the same pulse sequence (in our case we only have 18 T1-w images from the IBSR18 dataset). This function is used to correct for motion of the subject during the functional scans. Realignment results in changes to the (affine) transformation that is incorporated into the ".nii" files that are provided as input. Figure 3.2 shows the realign function from SPM12 and its parameters.

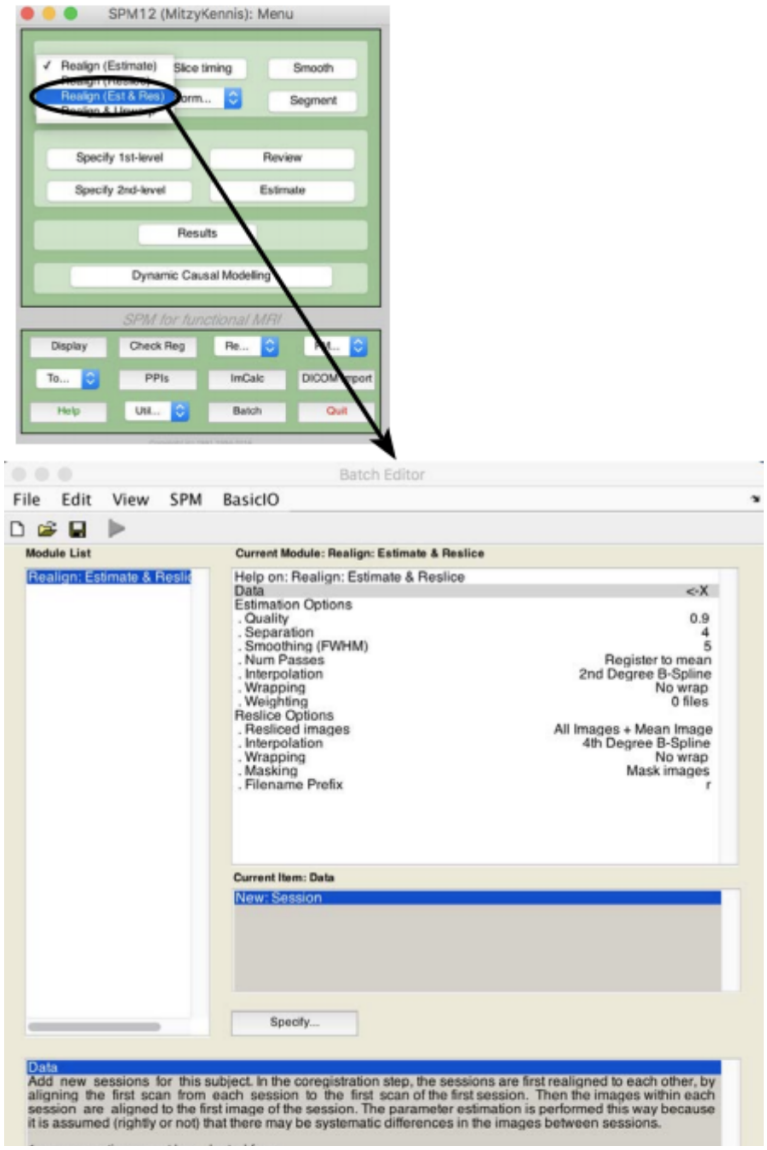

Figure 3.2: Realign function and parameters from SPM12

3.2.2 Segment Function

The second step on using SPM12 was to implement the segmentation function. It is important to mention that SPM12 upgraded segmentation function performs a spatially normalization, bias field correction and segmentation of tissues, all in the same function. Therefore, the pre-processing steps are already included when using the function by default. However they can be turned-off if the user would like to perform some other type of pre-processing techniques. Figure 3.3 shows the segmentation menu of SPM12 and its parameters.

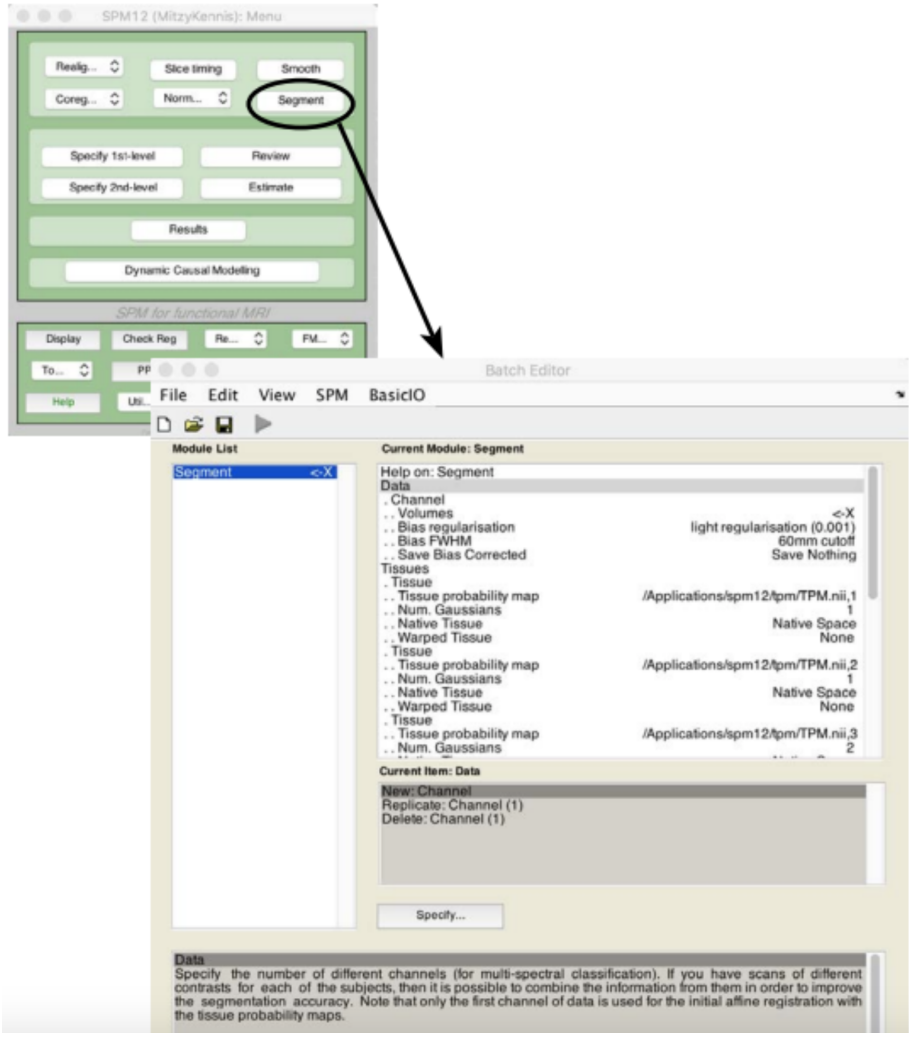

Figure 3.3: Segmentation function and parameters from SPM12

The segment function from SPM12 can be used to separate brain images into the following tissue classes: GM, WM, CSF, skull/bones, soft tissue and air/background (Figure 3.4. Segmentation is achieved by using tissue probability maps, which quantifies the probability of a pixel of belonging to a certain tissue type.

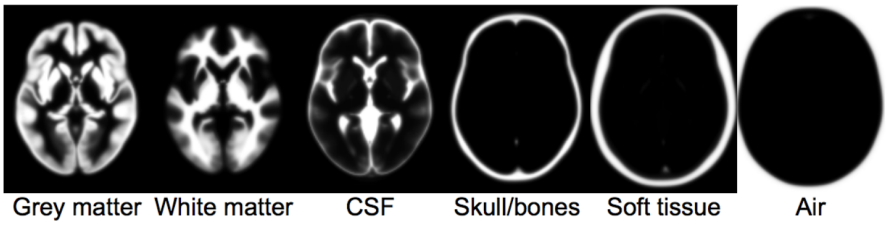

Figure 3.4: Brain tissue types segmented by SPM12

4. Experiments

4.1 Atlas based segmentation

The *IBSR* dataset provided had volumes with different voxel spacing and intensities but probabilistic atlas based segmentation completely depends on these two aspects and it requires the volumes to be in same voxel spacing and intensity ranges for all volumes. In order to achieve this the volumes needs to be heavily pre-processed and with right proportions of filters.

4.1.1 Test Runs

This section shows few of the main experiments done to check different combinations of pre-processing steps. Dice coefficient was used as the main metric to evaluate the results at all the steps.

Test 1 : No pre-processing

Table 4.1 shows the initial dice coefficients obtained on the validation set before any pre-processing was applied on the volumes.

Table 4.1: Dice Coefficients for Test 1

Volume	**CSF**	**GM**	**WM**
IBSR_11	0.6777	0.8158	0.7103
IBSR_12	0.7786	0.8535	0.8038
IBSR_13	0.7996	0.7739	0.7176
IBSR_14	0.8621	0.8384	0.8332
IBSR_17	0.8777	0.8809	0.8135

Test 2 : Anisotropic diffusion denoising

Denoising was required to make each tissue type homogeneous within the same volume and anisotropic filter was chosen because we also need to preserve the edges. Initially the filter was applied with more number of iterations which gave a very smooth homogeneous image but the final dice coefficient decreased because most of the minor detail were lost. So we chose to apply a very small denoising with only 2 iterations to preserve important details and at the same time to smooth large regions. Figures 4.1 and 4.2 shows the effect of applying anisotropic filtering with 2 and 5 iterations.

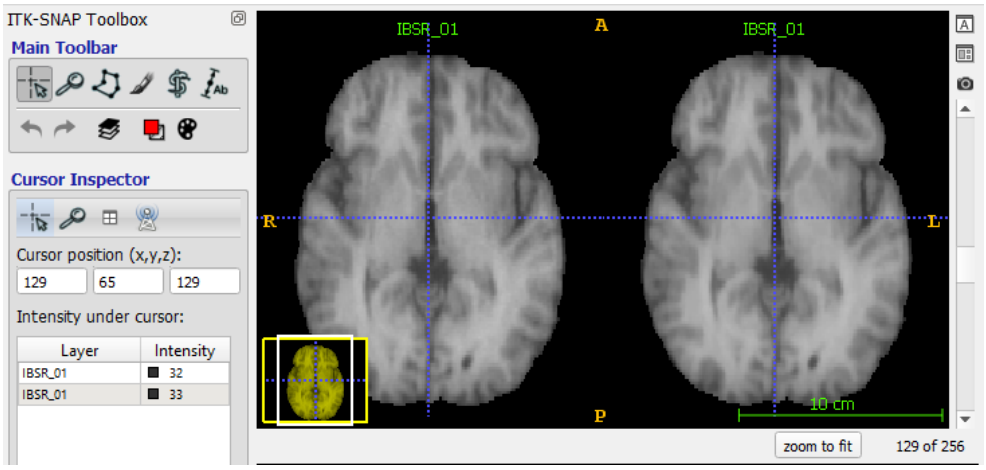

Figure 4.1: Illustration of anisotropic diffusion smoothing of *IBSR_01* with 2 iterations. Left(Original) and Right(Smoothed)

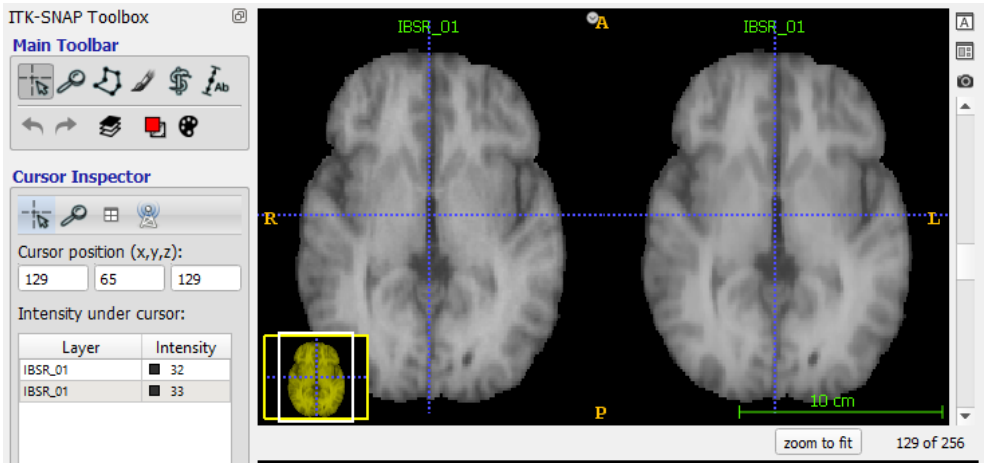

Figure 4.2: Illustration of anisotropic diffusion smoothing of *IBSR_01* with 5 iterations. Left(Original) and Right(Smoothed)

Test 3 : Histogram matching

It was observed that different volumes in the dataset had different intensity ranges, and so we chose to apply histogram matching with one volume *IBSR_07* which had good contrast and well defined boundaries between tissue types compared to the rest of the volumes. Figure 4.3 and 4.4 shows the histograms and the volumes with well defined boundaries and contrast enhanced after histogram matching.

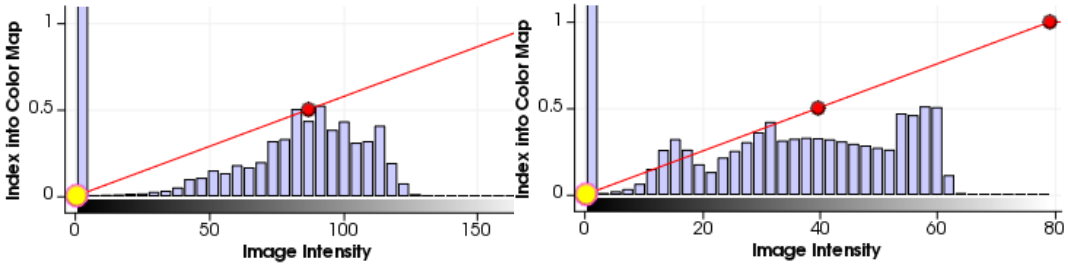

(a) Before matching (b) After matching

Figure 4.3: Illustration of histogram matching showing histograms of *IBSR_01*.

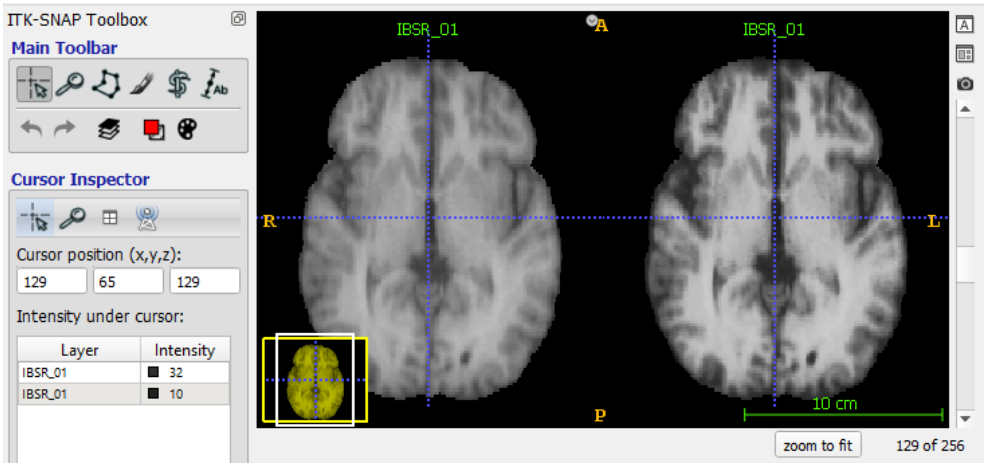

Figure 4.4: Illustration of histogram matching of *IBSR_01* with *IBSR_07*. Left(Original) and Right(Histogram matched)

Test 4 : Histogram stretching

From Test 3 it can be observed that even though the volume is well contrasted after histogram matching the intensity range of *IBSR_01* was very much decreased as the intensity range of *IBSR_07* was very less and in order to distribute the intensity range of the volumes it was decided to try histogram stretching, ranging from 256-1024. Finally 256 was observed to give better results compared to other ranges. Figures 4.5 and 4.6 shows the histograms and stretched image for *IBSR_07*. Since all the other volumes will be matched with this volume, the stretching was applied only to this volume.

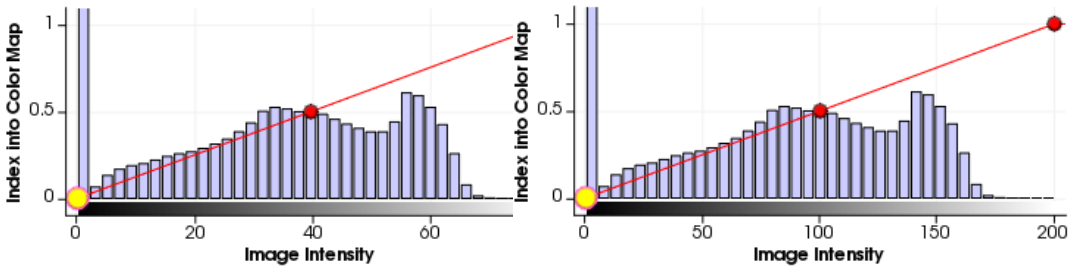

(a) Before stretching (b) After stretching

Figure 4.5: Illustration of histogram stretching showing histograms of *IBSR_07*.

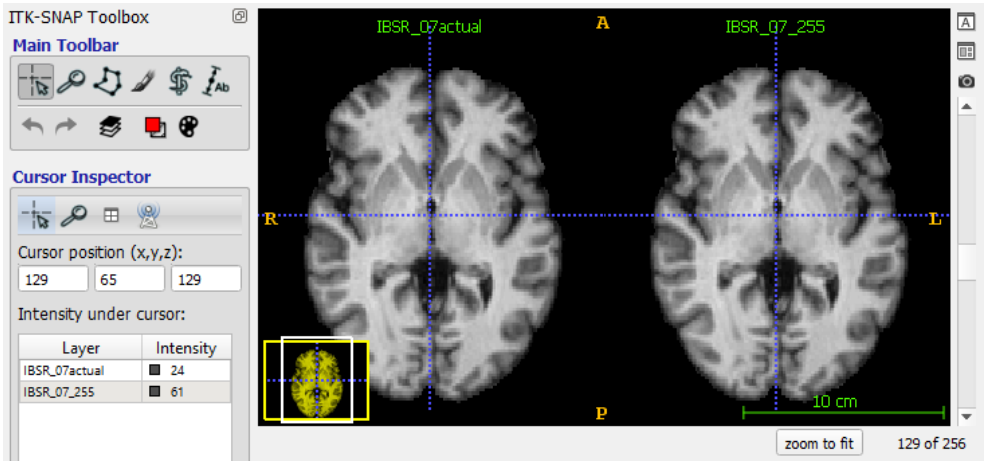

Figure 4.6: Illustration of histogram stretching of *IBSR_07*. Left(Original) and Right(Histogram stretched)

Test 5 : Combination of selected filters

This test was done with all the 3 combination of filters previously selected and taking into consideration different orders. It was decided that the below given order gives the best results compared to other combination of filters.

- Histogram stretching of *IBSR_07* from 0-200. When other volumes are matched with this volume few volumes will have intensities fall above 200 and so 200 was chosen so the intensity range for all the volumes can be considered from 0-255.
- Anisotropic diffusion denoising with 2 iterations.
- Histogram matching of all volumes with *IBSR_07*.

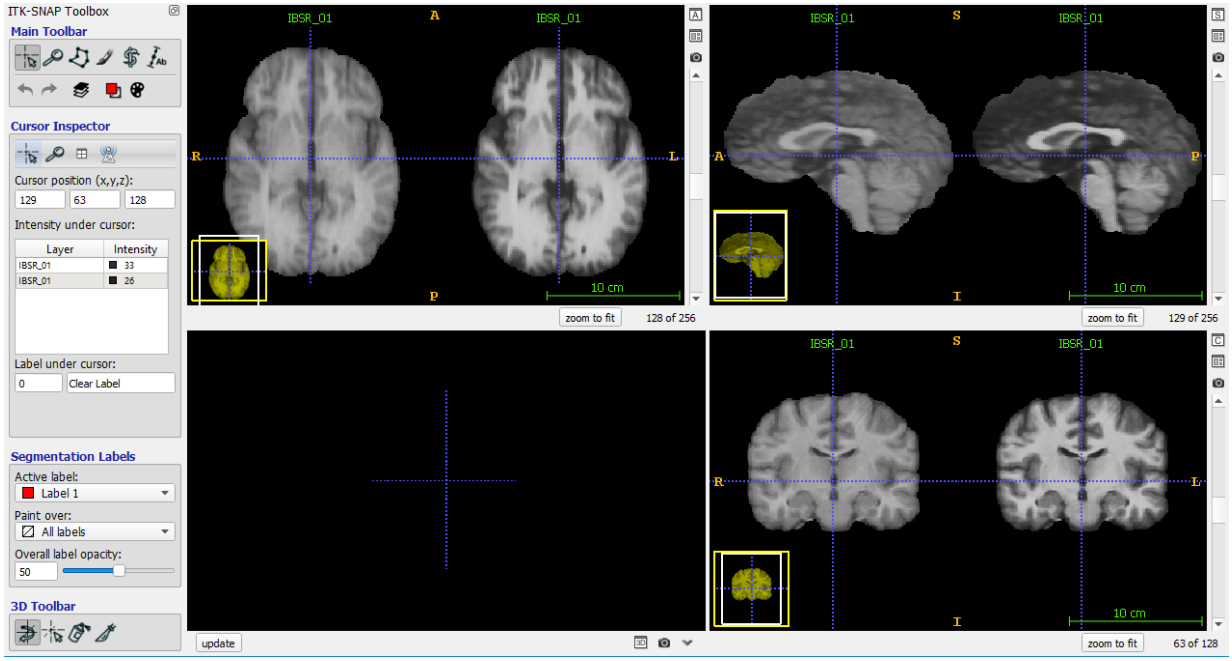

Figure 4.7: Illustration of all pre-processing steps applied on *IBSR_01*. Left(Original) and Right(Processed)

Other tests : Improve results

- Change registration interpolation order between $0-3$ -> Final order chosen *'0'*.
- Change BSpline registration physical pixel spacing between $8-32$mm. -> Final pixel spacing chosen 16mm.
- Apply N4ITK bias field correction -> No change in image quality hence discarded.

4.2 SPM12 segmentation

4.2.1 Test Runs

Test 1: Using SPM's tissue probability map

On our first attempt using SPM's 'Segment' function we tried to perform segmentation of the tissues by using the provided tissue probability maps that come by default. On the SPM12 documentation it is established that the 'Segment' function performs image alignment, spatially normalization and bias correction, all in the same model. However after performing our first attempt, we obtained the results shown in Figure 4.8:

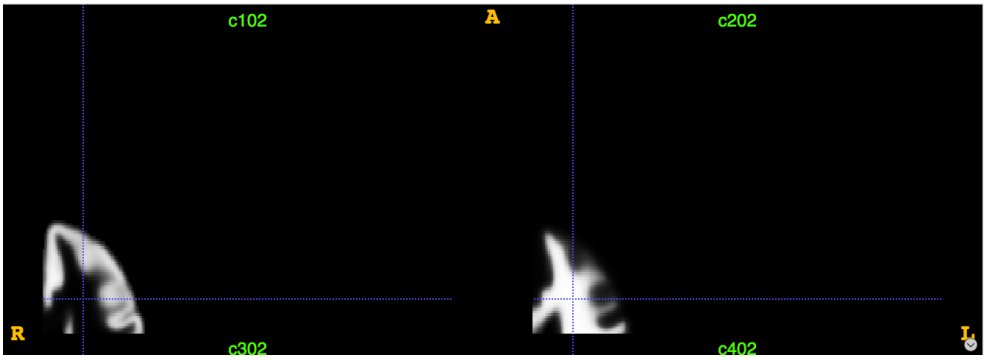

Figure 4.8: Using SPM's tissue probability map: first attempt

As the obtained results were cropped we assumed there was a problem regarding the registration of the images. Therefore we decided to apply the 'Realign' function first, followed by the 'Segment' function. The obtained results are shown in Figure 4.9:

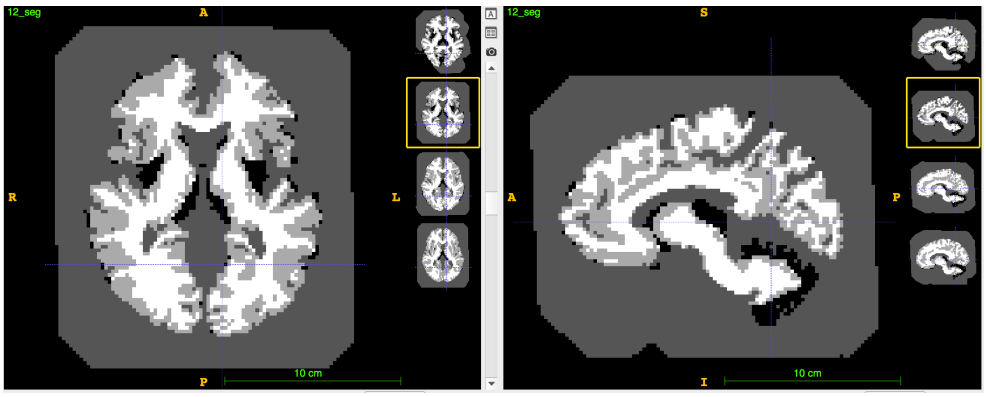

Figure 4.9: Using SPM's tissue probability map: second attempt

Test 2: Using our own probabilistic atlas

As the obtained results by using the provided tissue probability maps from SPM12 were far from good, we decided to try using the 'Segment' function but using our previously built probabilistic atlas. The segmentation improved greatly and we started to get some decent results as shown in Figure 4.14:

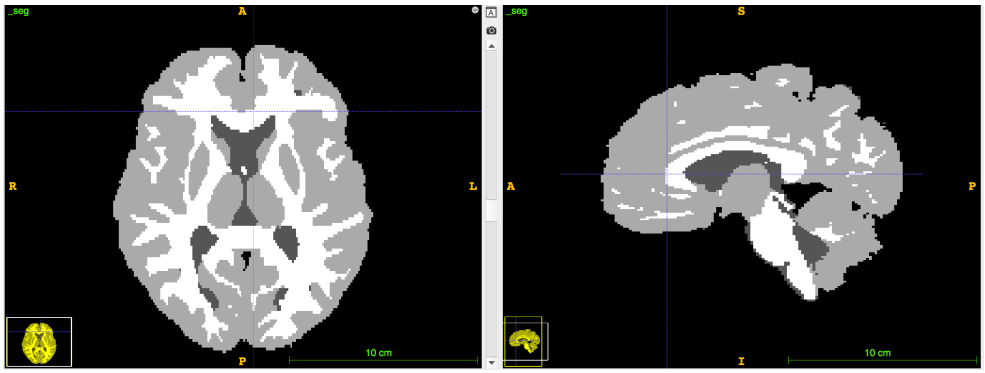

Figure 4.10: Using our own probabilistic atlas for brain tissue segmentation

After comparing the results obtained from Test 1 (using SPM's tissue probability maps) and Test 2 (using our own built atlas) it was clear that the way to proceed was by using our own atlas. Therefore the next tests were all performed with our built atlas and the only parameter that we were able to tune was the regularization of the bias field.

It is stated on the SPM manual that a more accurate estimate of a bias field can be obtained by including prior knowledge about the distribution of the fields likely to be encountered by the correction algorithm. Knowing what works best should be a matter of empirical exploration, for example, if the data has very little intensity non-uniformity artifact, then the bias regularization should be increased. This effectively tells the algorithm that there is very little bias in the data so it does not try to model it.

We performed some tests in order to find which bias regularization option was the most optimal for the IBSR18 dataset. The following bias regularization options were tested: light, medium, heavy and no regularization.

Test 3: No regularization (0)

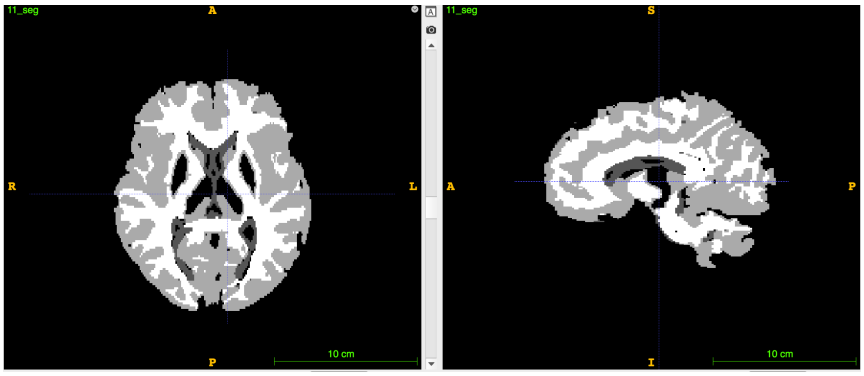

Figure 4.11: Segmentation results for Test 3: no regularization

Table 4.2: Mean Dice Coefficients for Test 3: no regularization

Volume	CSF	GM	WM
Validation set	0.3513	0.4367	0.6341

Test 4: Light regularization of the bias field (0.001)

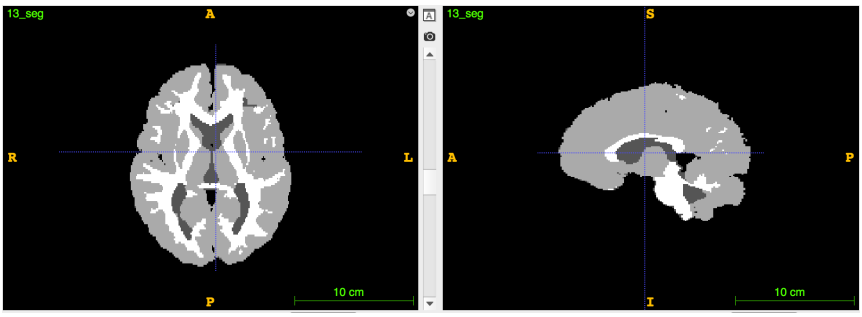

Figure 4.12: Segmentation results for Test 4: light regularization

Table 4.3: Mean Dice Coefficients for Test 4: light regularization

Volume	CSF	GM	WM
Validation set	0.3232	0.65536	0.58796

Test 5: Medium regularization of the bias field (0.01)

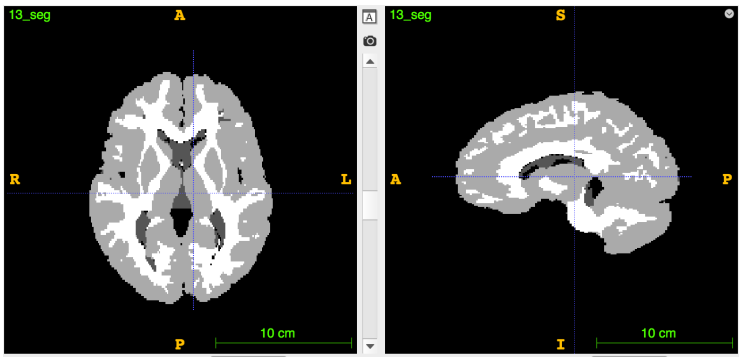

Figure 4.13: Segmentation results for Test 5: medium regularization

Table 4.4: Mean Dice Coefficients for Test 5: medium regularization

Volume	CSF	GM	WM
Validation set	0.25994	0.6481	0.5821

Test 6: Heavy regularization of the bias field (0.1)

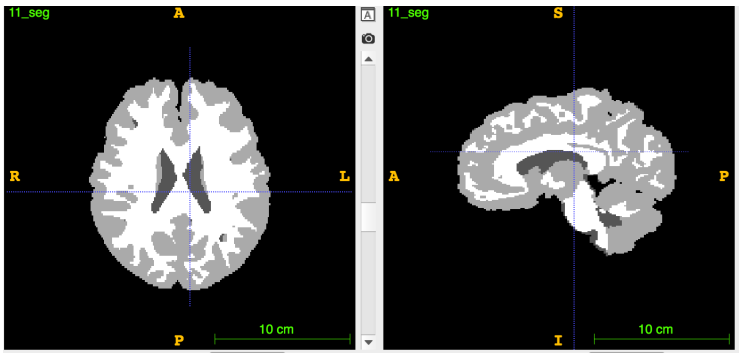

Figure 4.14: Segmentation results for Test 6: heavy regularization

Table 4.5: Dice Coefficients for Test 6: heavy regularization

Volume	CSF	GM	WM
Validation set	0.30194	0.4616	0.2429

From our testing we could observe that the most optimal bias parameter was using a light regularization (0.001) as it gave us the overall best Dice Coefficient values for the validation set.

However, when comparing the testing results from the atlas based segmentation against the segmentation using the SPM software, it is clearly visible that the atlas based segmentation is providing better results. Moreover, as this implementation was done from scratch there are several parameters that we could tune as well as pre and post processing that could be performed in order to enhance our results. Therefore, on the following section we provide the results obtained by performing atlas based segmentation only.

5. Results

This chapter provides the final quantitative and qualitative results obtained on the validation set using only Atlas based segmentation approach explained in the previous chapters and finally discuss on the obtained results.

5.1 Quantitative results

This section provides all the primary and secondary metrics calculated to evaluate the segmentation results on the validation set.

5.1.1 Dice Coefficient

Table 5.1: Dice Coefficient

Volume	**CSF**	**GM**	**WM**
IBSR_11	0.8222	0.8750	0.8950
IBSR_12	0.8447	0.8701	0.8990
IBSR_13	0.8232	0.8885	0.8507
IBSR_14	0.8621	0.9103	0.9063
IBSR_17	0.8855	0.9032	0.8702

5.1.2 Hausdorff Distance

Table 5.2: Hausdorff Distance

Volume	CSF	GM	WM
IBSR_11	33.3467	9.0000	7.5000
IBSR_12	28.2002	7.2801	7.8103
IBSR_13	10.4075	11.2952	10.5751
IBSR_14	27.7449	7.9572	9.4218
IBSR_17	26.4711	9.5014	11.7591

5.1.3 Average Distance

Table 5.3: Average Distance

Volume	CSF	GM	WM
IBSR_11	30.4834	15.6066	14.0751
IBSR_12	27.7287	17.5366	12.9197
IBSR_13	27.1702	14.7919	19.0030
IBSR_14	19.2985	10.4354	11.9083
IBSR_17	19.9657	11.0142	15.8752

5.1.4 Jaccard Coefficient

Table 5.4: Jaccard Coefficient

Volume	CSF	GM	WM
IBSR_11	0.6980	0.7778	0.8100
IBSR_12	0.7311	0.7700	0.8166
IBSR_13	0.6996	0.7994	0.7403
IBSR_14	0.7576	0.8353	0.8286
IBSR_17	0.7945	0.8235	0.7702

5.1.5 False Positive Error

Table 5.5: False Positive Error

Volume	CSF	GM	WM
IBSR_11	0.1271	0.0506	0.1364
IBSR_12	0.1896	0.0725	0.0834
IBSR_13	0.0999	0.1273	0.0620
IBSR_14	0.0566	0.0546	0.0979
IBSR_17	0.0800	0.0982	0.0795

5.1.6 False Negative Error

Table 5.6: False Negative Error

Volume	CSF	GM	WM
IBSR_11	0.2230	0.1886	0.0712
IBSR_12	0.1180	0.1806	0.1179
IBSR_13	0.2415	0.0951	0.2217
IBSR_14	0.2063	0.1224	0.0895
IBSR_17	0.1465	0.0954	0.1749

5.1.7 Volume Similarity

Table 5.7: Volume Similarity

Volume	CSF	GM	WM
IBSR_11	-0.1163	-0.1567	0.0728
IBSR_12	0.0846	-0.1238	-0.0383
IBSR_13	-0.1707	0.0362	-0.1861
IBSR_14	-0.1723	-0.0744	0.0093
IBSR_17	-0.0750	0.0031	-0.1092

5.2 Qualitative results

5.2.1 Segmentation Results - ITK Snap

In this section we present the visual segmentation results by displaying the original image, ground truth and segmentation result using the ITK Snap software.

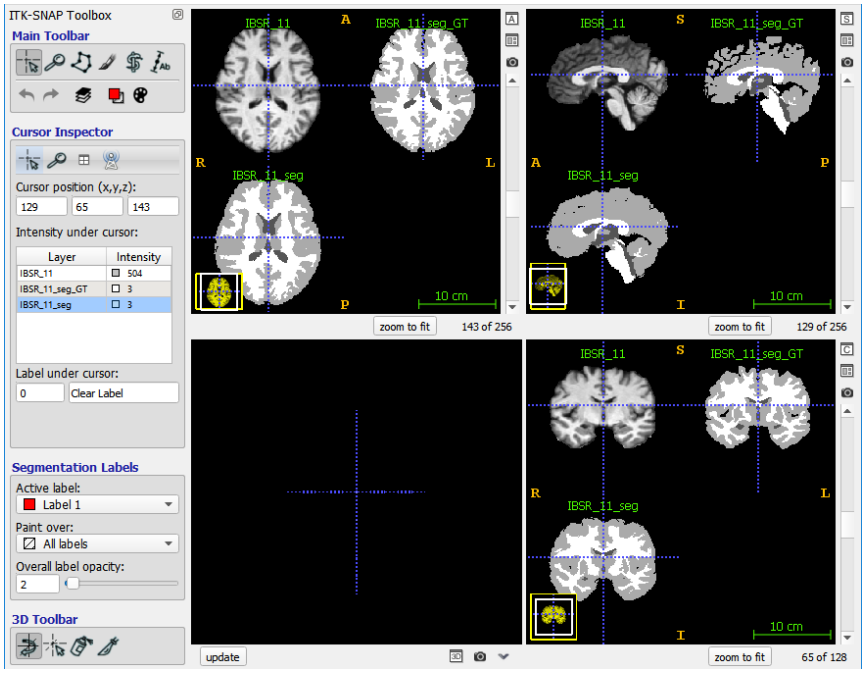

Figure 5.1: Segmentation result for IBSR_11. Top-left (Original image), Top-right (Segmentation ground truth), Bottom-left (Segmentation result).

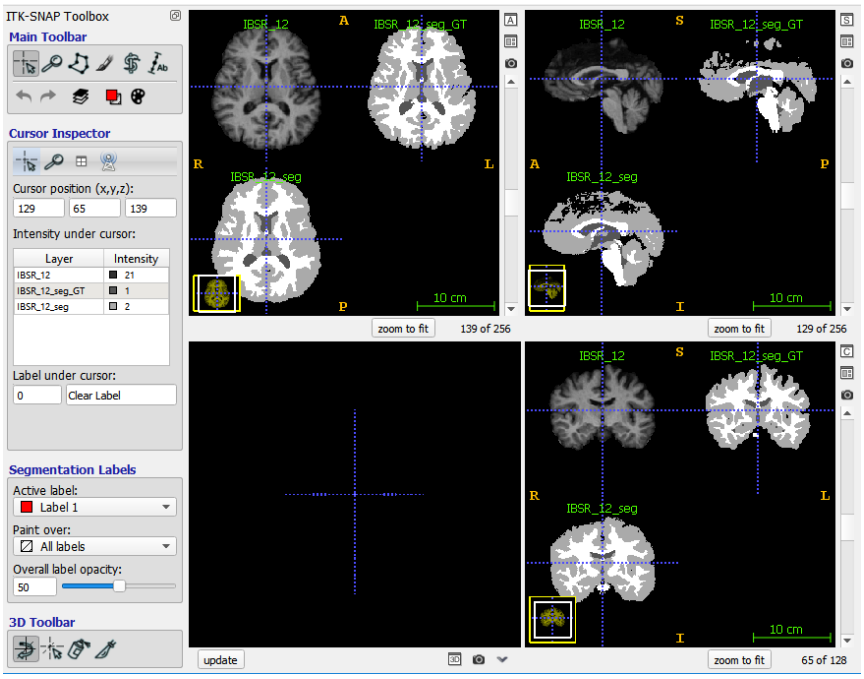

Figure 5.2: Segmentation result for IBSR_12. Top-left (Original image), Top-right (Segmentation ground truth), Bottom-left (Segmentation result).

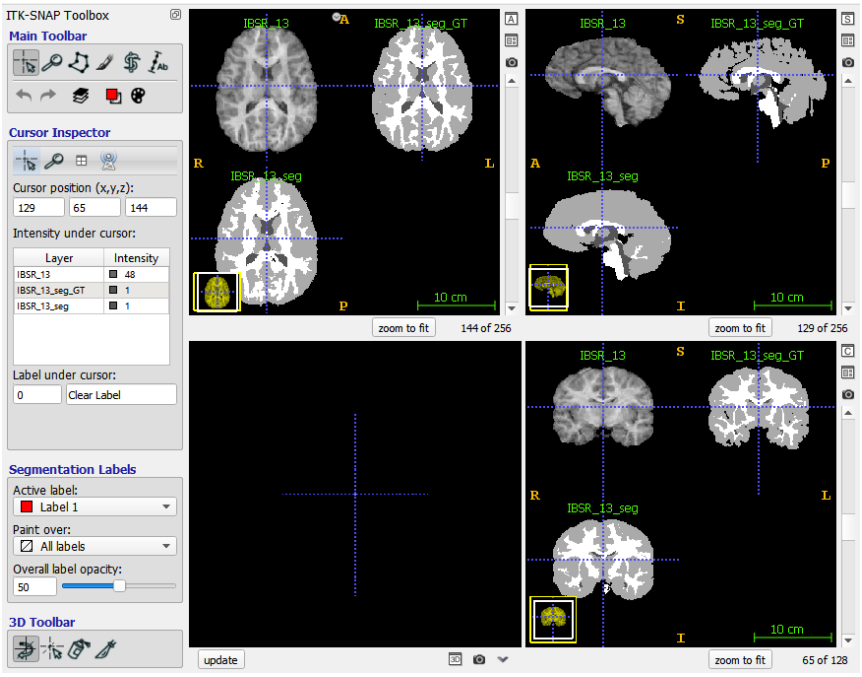

Figure 5.3: Segmentation result for IBSR_13. Top-left (Original image), Top-right (Segmentation ground truth), Bottom-left (Segmentation result).

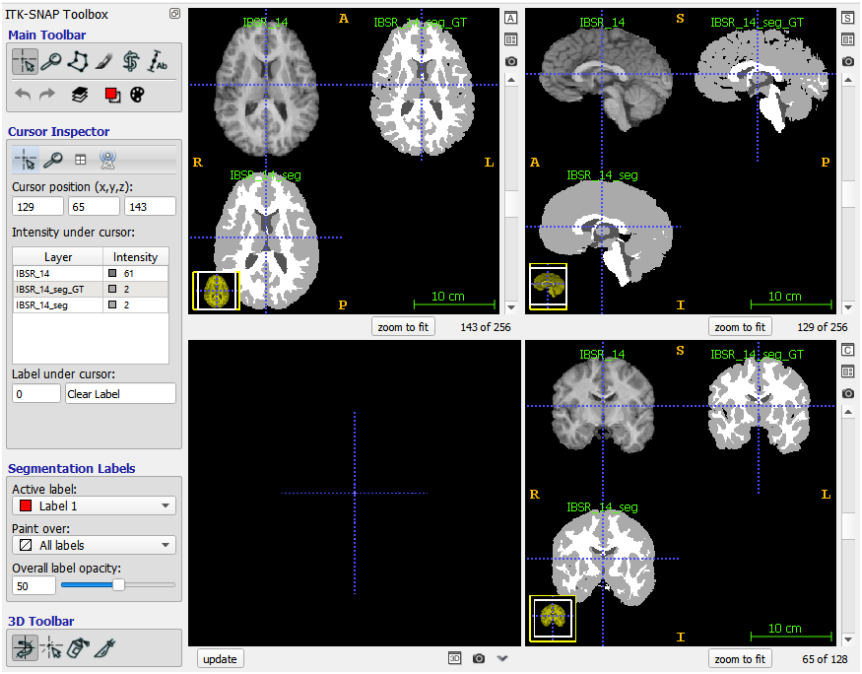

Figure 5.4: Segmentation result for IBSR_14. Top-left (Original image), Top-right (Segmentation ground truth), Bottom-left (Segmentation result).

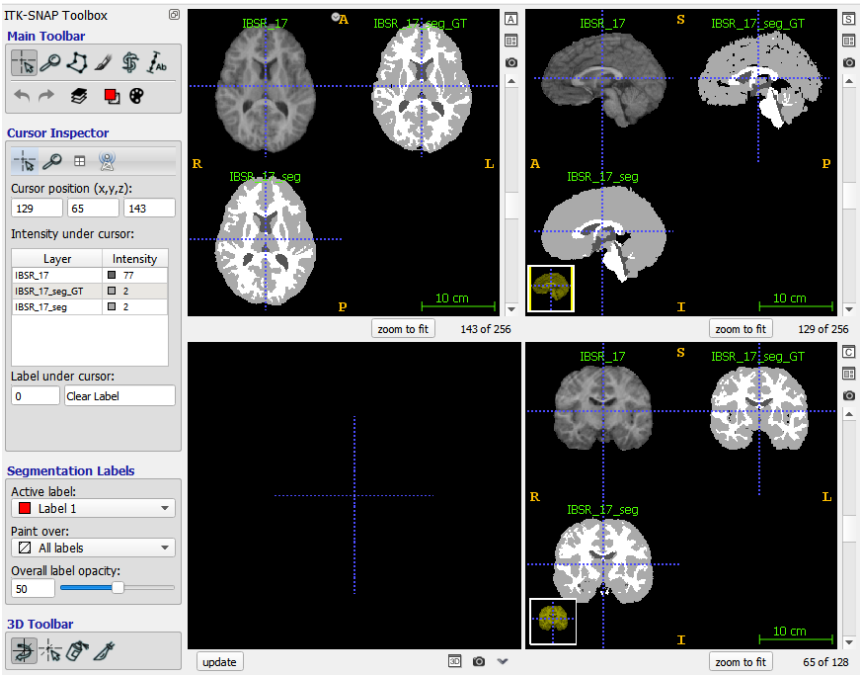

Figure 5.5: Segmentation result for IBSR_17. Top-left (Original image), Top-right (Segmentation ground truth), Bottom-left (Segmentation result).

5.2.2 Segmentation Volume Overlay - Slicer 3D

In this section we include the visual segmentation results by displaying ground truth image(left) and the ground truth image with segmentation image as overlay(right) using Slicer 3D software. The 3 classes are clearly identified by 3 different colours and their differences/errors are shown by lighter shades of the same colours of each class.

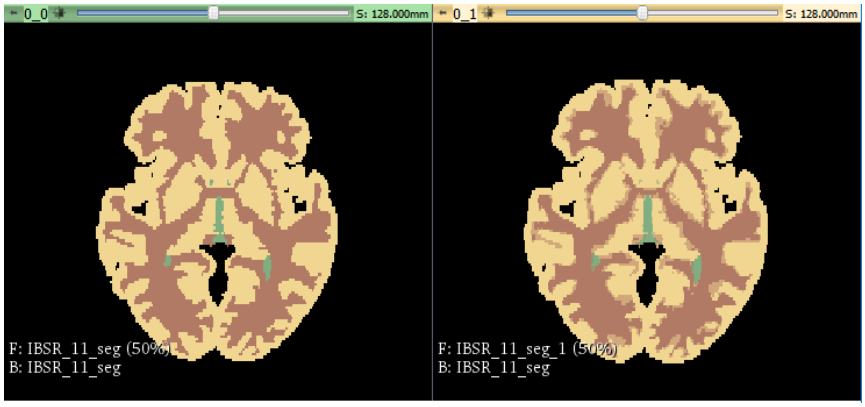

Figure 5.6: Illustration of segmentation volume overlay for IBSR_11. Left (Ground truth) and Right (Ground truth with segmentation result overlay of 50%).

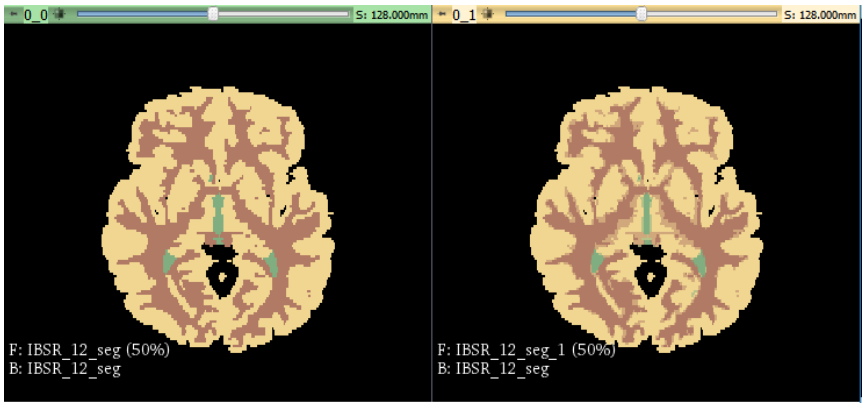

Figure 5.7: Illustration of segmentation volume overlay for IBSR_12. Left (Ground truth) and Right (Ground truth with segmentation result overlay of 50%).

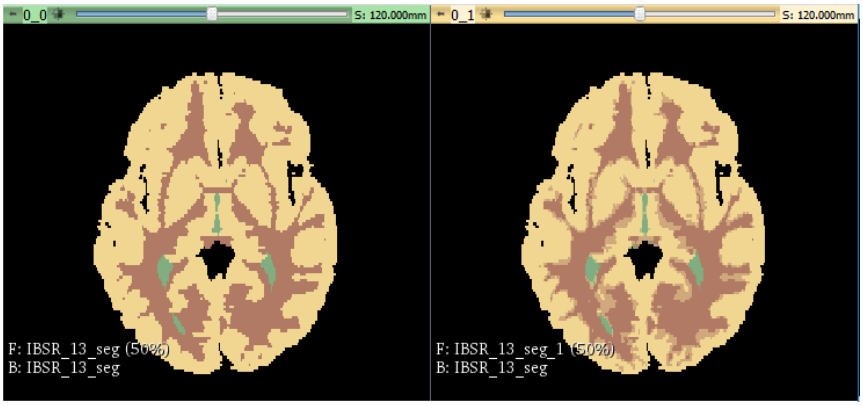

Figure 5.8: Illustration of segmentation volume overlay for IBSR_13. Left (Ground truth) and Right (Ground truth with segmentation result overlay of 50%).

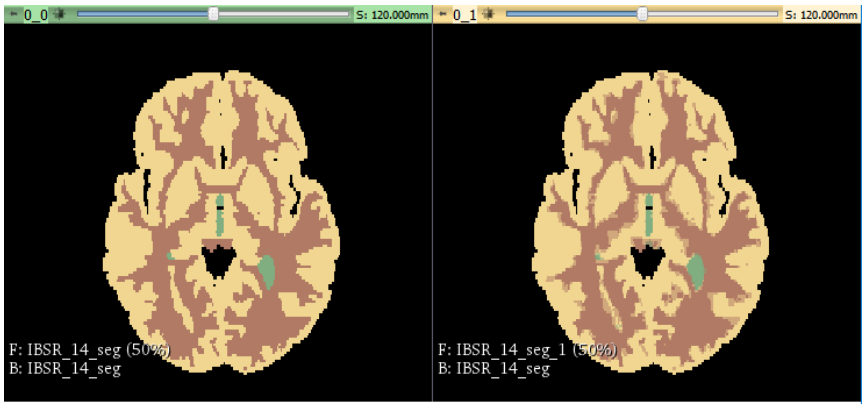

Figure 5.9: Illustration of segmentation volume overlay for IBSR_14. Left (Ground truth) and Right (Ground truth with segmentation result overlay of 50%).

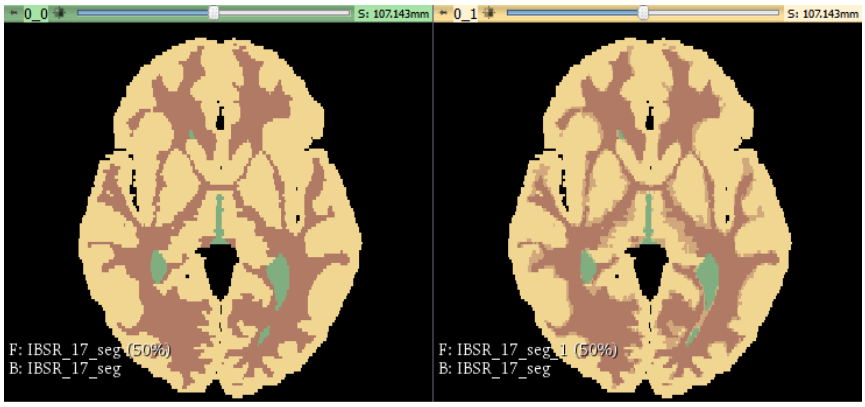

Figure 5.10: Illustration of segmentation volume overlay for IBSR_17. Left (Ground truth) and Right (Ground truth with segmentation result overlay of 50%).

5.2.3 Squared difference image

In this section we include the visual results of the squared difference between the ground truth images and the segmented images for individual classes. The visualization is done using ITK Snap and it is very easy to check for outliers and which type of tissue creates maximum false positives and false negatives when viewed along with the actual ground truth image.

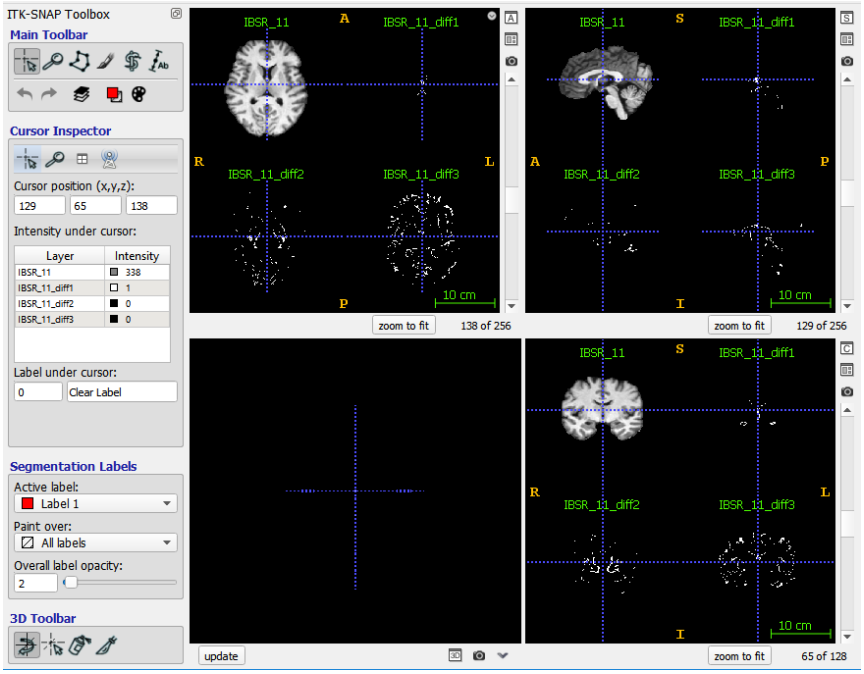

Figure 5.11: Squared difference of ground truth and segmentation for IBSR_11. Top-left (Original image), Top-right (CSF), Bottom-left (GM) and Bottom-right(WM).

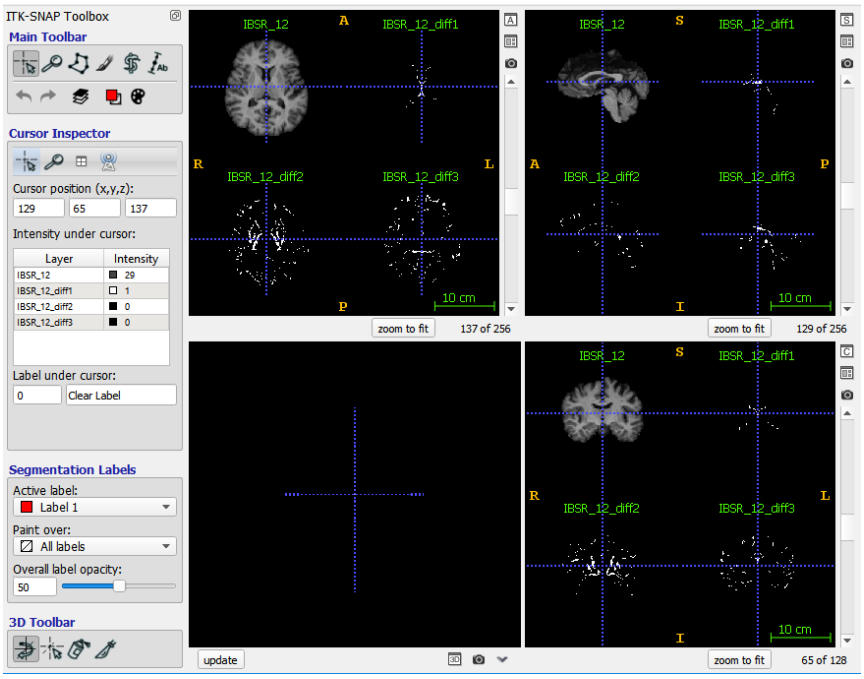

Figure 5.12: Squared difference of ground truth and segmentation for IBSR_12. Top-left (Original image), Top-right (CSF), Bottom-left (GM) and Bottom-right(WM).

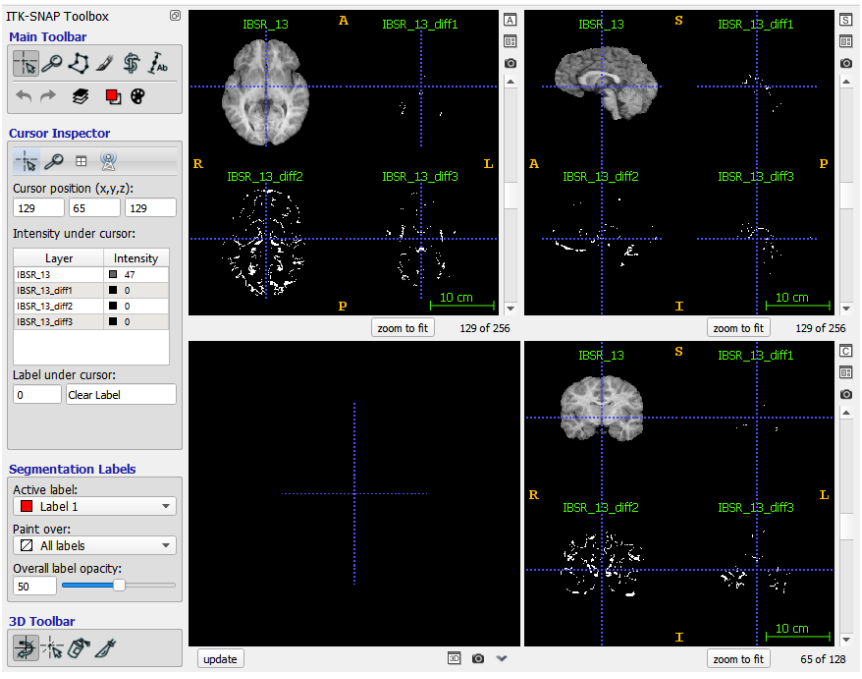

Figure 5.13: Squared difference of ground truth and segmentation for IBSR_13. Top-left (Original image), Top-right (CSF), Bottom-left (GM) and Bottom-right(WM).

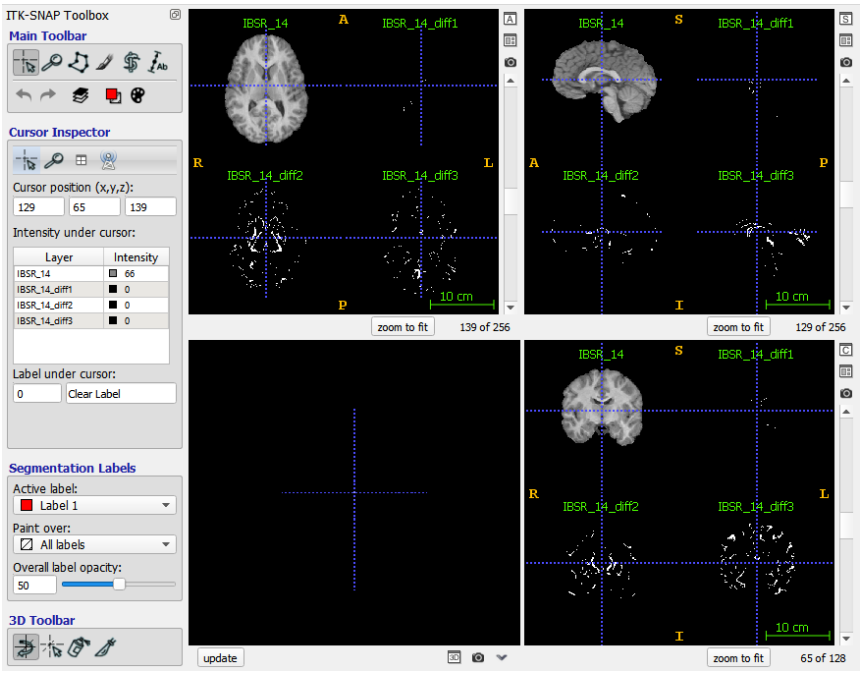

Figure 5.14: Squared difference of ground truth and segmentation for IBSR_14. Top-left (Original image), Top-right (CSF), Bottom-left (GM) and Bottom-right(WM).

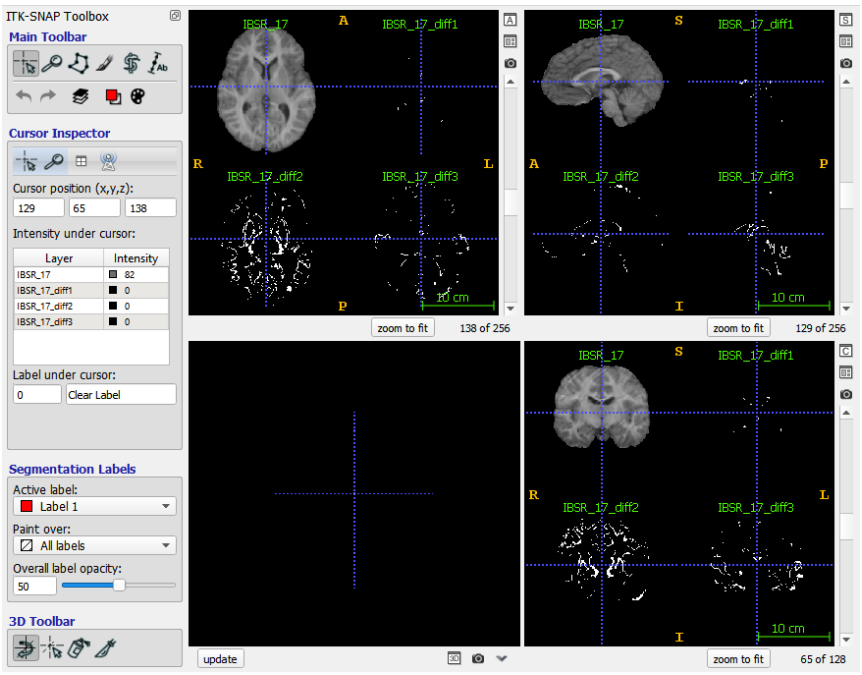

Figure 5.15: Squared difference of ground truth and segmentation for IBSR_17. Top-left (Original image), Top-right (CSF), Bottom-left (GM) and Bottom-right(WM).

5.3 Discussions

From the quantitative and qualitative results shown in the previous sections it can be observed that the the error is very high when segmenting the CSF class. One of the reasons being that the CSF is very small compared to the other classes and therefore, due to the partial volume effect between the CSF and GM it is easily mis-classified as GM. Since we are also using the background as a class during the segmentation and it does not have a proper distribution, some of the background pixels are also being considered as CSF and GM during the classification.

In addition to this, atlas based segmentation methods are highly dependent on the training volumes and it might not be possible to get a very high accuracy when the training and testing images are not very similar to each other. This is one of the main draw backs of the atlas segmentation method, which can be overcome by using different variants of atlas like using the cross-correlation to find the training images that are most similar to the test images and use only those images to get the final segmentation. But since the number of training images are not very high, it might not be always possible to find images that are highly correlated.

6. Project Management

We were given a total of 6 weeks for developing our implementation for the automatic segmentation challenge. The tasks performed each week are listed in the Table 6.1 and the hours dedicated by each of the team member is given in Table 6.2.

Table 6.1: Weekly tasks

Week	**Main Tasks**
Week 1	Define methods to approach objective Familiarize with the dataset Distribution of the project tasks
Week 2	Analyse various pre-processing techniques Familiarize with ITK, SPM
Week 3	Implement denoising with ITK Generate initial results using Atlas and SPM12 Analyze Slicer 3D & ITK for quantitative and qualitative results
Week 4	Implement histogram matching with ITK Implement histogram stretching using Matlab/ITK Analyze deep learning techniques
Week 5	Debug SPM12 tool Run tests to find different pre-processing final parameters Generate results on Test set
Week 6	Implement Markov Random Field to improve results Write report

Table 6.2: Working hours

Team Member	**Tasks**	**Week 1-2**	**Week 3-4**	**Week 5-6**
Umamaheswaran	Learning	8	10	2
	Coding	6	8	6
	Experiments	5	15	8
	Report	0	0	20
Katherine	Learning	10	8	4
	Coding	4	2	1
	Experiments	0	5	16
	Report	0	0	20

7. Conclusions

In this project, two approaches were mainly followed for performing the automatic segmentation task, first, using atlas based segmentation and second, using the open source software called SPM. The final implementation was performed using atlas based segmentation as we were more familiarized with the theory behind it and it also provided better segmentation results.

The implementation was done from scratch and further pre-processing and post-processing was developed. By adding more pre-processing techniques, such as denoising, histogram matching and histogram stretching, the results greatly improved.

The evaluation of our proposed atlas based segmentation algorithm was performed on the validation set and test set from the IBSR18 dataset. The final mean Dice Similarity Coefficients on validation set was CSF (0.848), GM (0.890) and WM (0.884) and on test set was CSF (0.834), GM (0.938) and WM (0.897). The results obtained were good and comparable with deep learning techniques followed by other team members. The overall standard deviation on each tissue was also very low, implying that our method is quite stable.

Further developments could be done to the proposed method in order to improve the obtained results. One of this improvements could be to finalize the implementation of the Markov Random Field code as it was still under development. Based on the experiments and the results shown in this report, it is likely that our segmentation would improve by adding this post processing technique to our algorithm.

Bibliography

[Akselrod-Ballin 2007] Ayelet Akselrod-Ballin, Meirav Galun, John Moshe Gomori, Achi Brandt et Ronen Basri. *Prior knowledge driven multiscale segmentation of brain MRI.* In International Conference on Medical Image Computing and Computer-Assisted Intervention, pages 118–126. Springer, 2007.

[Ashburner 2005] John Ashburner et Karl J Friston. *Unified segmentation.* Neuroimage, vol. 26, no. 3, pages 839–851, 2005.

[Cabezas 2011] Mariano Cabezas, Arnau Oliver, Xavier Lladó, Jordi Freixenet et Meritxell Bach Cuadra. *A review of atlas-based segmentation for magnetic resonance brain images.* Computer methods and programs in biomedicine, vol. 104, no. 3, pages e158–e177, 2011.

[Cuadra 2015] M Bach Cuadra, V Duay et J-Ph Thiran. *Atlas-based segmentation.* In Handbook of Biomedical Imaging, pages 221–244. Springer, 2015.

[Gonzalez 2002] Rafael C Gonzalez, Richard E Woods*et al. Digital image processing*, 2002.

[Held 1997] Karsten Held, E Rota Kops, Bernd J Krause, William M Wells, Ron Kikinis et H-W Muller-Gartner. *Markov random field segmentation of brain MR images.* IEEE transactions on medical imaging, vol. 16, no. 6, pages 878–886, 1997.

[Jaccard 1912] Paul Jaccard. *The distribution of the flora in the alpine zone.* New phytologist, vol. 11, no. 2, pages 37–50, 1912.

[Jain 1989] Anil K Jain. Fundamentals of digital image processing. Prentice-Hall, Inc., 1989.

[Kalinić 2009] Hrvoje Kalinić. *Atlas-based image segmentation: A Survey.* 2009.

[Kapur 1996] Tina Kapur, W Eric L Grimson, William M Wells et Ron Kikinis. *Segmentation of brain tissue from magnetic resonance images.* Medical image analysis, vol. 1, no. 2, pages 109–127, 1996.

[Perona 1990] Pietro Perona et Jitendra Malik. *Scale-space and edge detection using anisotropic diffusion.* IEEE Transactions on pattern analysis and machine intelligence, vol. 12, no. 7, pages 629–639, 1990.

[Phillips 2015] Jennifer L Phillips, Lisa A Batten, Philippe Tremblay, Fahad Aldosary et Pierre Blier. *A prospective, longitudinal study of the effect of remission on cortical thickness and hippocampal volume in patients with treatment-resistant depression.* International Journal of Neuropsychopharmacology, vol. 18, no. 8, page pyv037, 2015.

[Sun 2015] Xiaofei Sun, Lin Shi, Yishan Luo, Wei Yang, Hongpeng Li, Peipeng Liang, Kuncheng Li, Vincent CT Mok, Winnie CW Chu et Defeng Wang. *Histogram-based normalization technique on human brain magnetic resonance images from different acquisitions.* Biomedical engineering online, vol. 14, no. 1, page 73, 2015.

[Taha 2015] Abdel Aziz Taha. *Addressing metric challenges: Bias and Selection Efficient Computation Hubness Explanation and Estimation.* PhD thesis, Dissertation, Vienna University of Technology, 2015.

[Tustison 2009] NJ Tustison et JC Gee. *Introducing Dice, Jaccard, and other label overlap measures to ITK.* Insight J, pages 1–4, 2009.